American Mineralogist, Volume 84, pages 1152–1161, 1999

Crystal structure of boralsilite and its relation to a family of boroaluminosilicates, sillimanite, and andalusite

DONALD R. PEACOR,[1],* ROLAND C. ROUSE,[1] AND EDWARD S. GREW[2]

[1]Department of Geological Sciences, The University of Michigan, Ann Arbor, Michigan 48109, U.S.A.
[2]Department of Geological Sciences, University of Maine, Orono, Maine 04469, U.S.A.

ABSTRACT

Boralsilite, $Al_{16}B_6Si_2O_{37}$, is monoclinic, space group $C2/m$, with a = 14.767(1), b = 5.574(1), c = 15.079(1) Å, β = 91.96(1)°, and Z = 2. The structure was solved with direct methods and refined to an unweighted residual of 0.026 using 1193 observed reflections. The structure is closely related to those of sillimanite, andalusite, grandidierite, synthetic aluminum borate ($Al_{18}B_4O_{33}$), and werdingite. These structures are all based on a backbone of chains of edge-sharing AlO_6 octahedra arranged parallel to c ($\cong$ 5.6 Å) and at the vertices and center of a pseudo-tetragonal subcell having $a \cong b \cong 7.5$ Å. In the boralsilite structure, AlO_6 octahedral chains are cross-linked by Si_2O_7 disilicate groups, BO_4 tetrahedra, BO_3 triangles, and AlO_5 trigonal bipyramids. A given BO_4 or SiO_4 tetrahedron or BO_3 triangle shares two vertices with two adjacent AlO_6 octahedra of one chain and a third vertex with an octahedron vertex of an adjacent chain, thus cross-linking the AlO_6 octahedral chains. Further linkage is provided through vertex-sharing of AlO_5 trigonal bipyramids. These bipyramids alternate with B or Si polyhedra parallel to AlO_6 octahedral chains to form four kinds of cross-linking chains of polyhedra, with alternate atom pairs $^{[5]}$Al1-Si, $^{[5]}$Al2-$^{[4]}$B2, $^{[5]}$Al3-$^{[3]}$B1, and $^{[5]}$Al4-$^{[3]}$B3. The units which cross-link between chains of AlO_6 octahedra can alternatively be viewed as consisting of Si_2O_7 dimers, trimers of edge-sharing AlO_5 trigonal bipyramids (plus a B triangle and B tetrahedron), and dimers of edge-sharing AlO_5 trigonal bipyramids (plus B triangles and tetrahedra), Variations on these themes are found in the structures of sillimanite, andalusite, grandidierite, werdingite, mullite, and synthetic $Al_{18}B_4O_{33}$. The interchangeability and variety of the various interchain units appears to result in part from the flexibility produced by the ability of Al and B to assume a variety of coordinations by oxygen and from the potential for partial vacancy of some anion and cation sites.

INTRODUCTION

Boralsilite ($Al_{16}B_6Si_2O_{37}$) was described as a new mineral by Grew et al. (1998), in part based on the results of the crystal structure analysis that is described in detail here. Its structure is closely related to that of sillimanite and thus to a large group of aluminosilicates and boroaluminosilicates which includes sillimanite, andalusite, mullite, werdingite, grandidierite, and synthetic aluminum borate ($Al_{18}B_4O_{33}$) (Table 1). All of these phases have closely related structures based on similar arrays of chains of edge-sharing AlO_6 octahedra. The relation between boralsilite and these phases is suggested not only by similarities in composition and lattice parameters, but also by parallel intergrowths of boralsilite with werdingite and grandidierite and by a scalariform (ladder-like) werdingite-boralsilite intergrowth resembling textures derived through exsolution.

It is well known that the crystal structures of andalusite and sillimanite (Burnham and Buerger 1961; Burnham 1963) are based on a common theme of chains of edge-sharing Al-octahedra oriented parallel to the c-axis, chains that have (x,y) coordinates (0,0) and (1/2,1/2) and that are linked by fourfold- or fivefold-coordinated Al and tetrahedrally coordinated Si. The mullite structure, for which there is a range of solid solution, is derivative to the sillimanite structure, but it retains the octahedral chains virtually unchanged. Synthetic ternary solid solutions with compositions between those of mullite and Si-free aluminum borates, and apparently having the same basic unit of structure as sillimanite, have been called "boron-mullites" (Werding and Schreyer 1984; 1996; Grew et al. 1998). The structure of synthetic Al borate, whose composition is given variously as Al_5BO_9 and $Al_{18}B_4O_{33}$, also has octahedral chains cross-linked by units related to those in sillimanite, andalusite, and mullite (Sokolova et al. 1978; Ihara et al. 1980; Garsche et al. 1991). The structures of the Fe- and Mg-bearing minerals werdingite, $Al_8[(Mg,Fe)_2Al_4(Al,Fe)_2Si_4(B,Al)_4]O_{37}$, and grandidierite, $Al_2[AlMgBSi]O_9$, have similar subunits, with cross-linking polyhedra which display even greater variety due to the presence of Mg and Fe.

Table 1 summarizes the compositions and unit-cell data for the relevant phases whose structures have been determined. A translation of approximately 2.8 Å or multiples thereof reflects periodicity in the chain of AlO_6 octahedra, one octahedron having an O-O edge approximately 2.8 Å in length. Similarly, the simple relations between the values of the cell dimensions within the plane perpendicular to the chains of octahedra are a measure of the distribution of chains in this plane; i.e., with coordinates (0,0) and (1/2,1/2) relative to a cell with $A \cong B \cong 7.5$ Å.

---

*E-mail: drpeacor@umich.edu

0003-004X/99/0708–1152$05.00

TABLE 1. Compositions and crystallographic data for phases with structures related to that of boralsilite

Name	Composition*	*Z*	Sp.Gp.	*a*	*b*	*c* (Å)	α	β	γ (°)
Sillimanite†	$Al[AlSi]O_5$	4	*Pbnm*	7.4586(6)	7.6738(3)	5.7698(8)			
Andalusite‡	$Al[AlSi]O_5$	4	*Pnnm*	7.7942(2)	7.8985(2)	5.559(2)			
Grandidierite§	$Al_2[(Fe,Mg)AlSiB]O_9$	4	*Pbnm*	10.335(2)	10.978(2)	5.760(2)			
Werdingite||	$Al_8[Mg,Fe)_2Al_4(Al,Fe)_2Si_4(B,Al)_4]O_{37}$	1	*P*1	7.995(2)	8.152(1)	11.406(4)	110.45(2)	110.85(2)	84.66(2)
A_9B_2(synthetic)#	$Al_8[(Al,B)_{12}B_4]O_{33}$	1	*A*2$_1$*am*	7.6942(1	15.0110(2	5.6689(1)			
Mullite**	$Al_2[Al_{2+2x}Si_{2-2x}]O_{10-x}$	1	*Pbam*	7.5785(6)	7.6817(7)	2.8864(3)			
Boralsilite††	$Al_8[Al_8B_6Si_2]O_{37}$	2	*C*2/*m*	14.767(1)	5.574(1)	15.079(1)		91.96(1)	

* Compositions are written so that Al of chains of edge-sharing octahedra are given first. Multiplication by a factor giving eight Al atoms in the chains normalizes formulae to a common structural basis.

† Burnham (1963).

‡ Burnham and Buerger (1961).

§ Stephenson and Moore (1968).

|| Niven et al. (1991).

A_9B_2 Garsche et al. (1991).

** Angel and Prewitt (1986); Data for average structure with x = 0.40.

†† Grew et al. (1998).

The lattice parameters of boralsilite, as initially determined using precession and Weissenberg photographs, implied a similar structural theme, but with the octahedral chains oriented parallel to *b* rather than *c* as necessitated by indexing of the cell using the second monoclinic setting. We therefore undertook a solution of the structure to determine its apparently unique scheme of chain cross-linking. Our overall aim was to construct a general scheme of structural relations through comparison of the boralsilite structure with those of the other closely related phases.

STRUCTURE SOLUTION AND REFINEMENT

Although twinning on {100} is ubiquitous, one small cleavage fragment from the Larsemann Hills, Antarctica, was found to be untwinned by this law, and it was therefore used for measurement of intensity data with an Enraf-Nonius CAD4 4-circle diffractometer. Relevant experimental details are listed in Table 2. The refined unit-cell parameters reported in Table 1 were determined using the optimized setting angles of 25 reflections. Extinctions confirmed that the space group is *C*2, *Cm*, or *C*2/*m*, and the last was subsequently determined to be correct by the structure analysis, which was carried out using the Enraf-Nonius crystallographic software system MolEN. Of the 1609 reflections whose intensities were measured, 1568 were unique and 1193 of those were considered "observed" at the $I > 2\sigma(I)$ threshold. The direct methods program MULTAN11/82 was used to determine the structure, centrosymmetry being implied by statistical analysis. Assuming space group *C*2/*m*, the locations of all atoms except B3 were revealed by the *E*-map. That atom was subsequently located by means of a difference electron-density synthesis. Refinement of the full set of atoms with isotropic displacement factors converged to weighted and unweighted residuals of 0.033 and 0.044, respectively.

TABLE 2. Experimental details

Crystal size	0.039 mm × 0.047 mm x 0.172 mm
Radiation	Monochromatized MoKα at 50 kV and 30 mA
Data measurement	
Index limits	$-18 \leq h \leq 18$, $0 \leq k \leq 7$, $0 \leq l \leq 19$
Maximum 2θ	54.90°
Scan type	ω- 2θ
Scan rates	Between 0.4° and 5.5°/min in ω
Scan widths	0.75 + 0.35tanθ in ω (°)
Intensity monitoring	3 reflections every 3 h
Orientation monitoring	3 reflections every 400 reflections
Data corrections	Lorentz-polarization and absorption (by the ψ-scan method using 6 reflections)
Refinement	
Type	Full-matrix least-squares
Function minimized	$Sw(\|F_{obs}\| - \|F_{cal}\|)^2$
Reflection weights	$4F^2_{obs}/[s(F^2_{obs})]^2$
Anomalous dispersion	For all atoms
Observations	1193 reflections [$I > 2\sigma(I)$]
Variables	173 refined parameters
R (observed data)	0.026
wR (observed data)	0.035
R (all data)	0.055
Esd obs. of unit weight	1.401
Largest shift/error	0.01

At this point it was apparent that the displacement factor of atom O10 consistently refined to a value two to three times larger than that of any other anion in the structure and a persistent feature of every difference Fourier synthesis was a small positive maximum of 1.5 e/Å^3 at (1/2,0,0), about 1.1 Å from atom O10. All other maxima were <0.5 e/Å^3. The residual at (1/2,0,0) was initially assumed to represent H, but that possibility was rejected because its displacement factor refined to –2.7(6) Å^2, implying a significantly higher concentration of electron density on that site and its presence would imply the existence of a perfectly linear and symmetrical H bond O10...H...O10', a phenomenon rarely encountered in crystals of inorganic compounds.

An alternative model, which considers the peak in question to be part of a "split" atom pair, i.e., O10A on equipoint 4*i* (0.444,0,0.049) and O10B on equipoint 2*b* (1/2,0,0), gave a more reasonable result. Treating the pair as two independent sites and refining their occupancy factors yielded values of 3.80(3) and 0.29(2) atoms for O10A and O10B, respectively. This variation in the overall boralsilite model produced only minor reductions in the residuals to 0.032 and 0.041, but this was to be expected given the very small amount of X-ray scattering power involved.

Finally, an attempt was made to refine the structure in space group *Cm*. The resulting residual was 0.031, but the refinement would not converge owing to very high correlations between atoms that are symmetrically equivalent in space group *C*2/*m*. No refinement was attempted in space group *C*2 as the same result was predicted. Boralsilite is therefore inferred to be centrosymmetric to the extent that this property can be de-

TABLE 3. Atomic positional parameters and equivalent isotropic displacement factors (Å^2)

Atom		*x*	*y*	*z*	*B*eq
Al1	4i	0.86873(7)	0	0.33837(7)	0.42(2)
Al2	4i	0.81194(7)	0	0.15838(7)	0.40(2)
Al3	4i	0.57170(7)	0	0.06951(7)	0.51(2)
Al4	4i	0.67697(7)	0	0.34140(7)	0.40(2)
Al5	8j	0.00396(5)	0.74670(13)	0.24322(5)	0.43(1)
Al6	4e	1/4	1/4	0	0.39(2)
Al7	4f	1/4	1/4	1/2	0.41(2)
Si	4i	0.42541(7)	0	0.41917(7)	0.42(2)
B1	4i	0.1018(3)	0	0.1009(3)	0.66(7)
B2	4i	0.3774(3)	0	0.1192(3)	0.69(7)
B3	4i	0.1356(3)	0	0.3633(3)	0.54(7)
O1	4i	0.7658(2)	0	0.2671(2)	0.59(4)
O2	4i	0.7965(2)	0	0.4340(2)	0.53(4)
O3	4i	0.9244(2)	0	0.2214(2)	0.41(4)
O4	8j	0.9355(1)	0.7387(3)	0.3573(1)	0.63(3)
O5	2d	0	1/2	1/2	0.90(7)
O6	4i	0.3234(2)	0	0.4584(2)	0.55(4)
O7	8j	0.8208(1)	0.7151(4)	0.1063(1)	0.57(3)
O8	4i	0.6973(2)	0	0.0613(2)	0.49(4)
O9	8j	0.0680(1)	0.7843(3)	0.1333(1)	0.58(3)
O10A	4i	0.4444(2)	0	0.0494(2)	0.98(5)
O10B	2b	0	1/2	0	2.7(7)
O11	8j	0.6678(1)	0.2877(4)	0.3991(1)	0.57(3)
O12	4i	0.5757(2)	0	0.2812(2)	0.50(4)
O13	4i	0.4313(2)	0	0.2005(2)	0.57(4)
O14	4i	0.0767(2)	0	0.2927(2)	0.49(4)
O15	4i	0.8314(2)	0	0.9594(2)	0.51(4)

Note: Atom O10B was refined using an isotropic displacement factor. The refined site occupancy factors of O10A and O10B are 3.80(3) and 0.29(2) atoms, respectively.

TABLE 6. Selected interatomic distances (Å) and bond angles (°).

AlO$_5$ Bipyramids			
Al1-O4	1.776(2) ×2	Al2-O7	1.779(2) ×2
O2	1.822(3)	O1	1.796(3)
O1	1.831(3)	O3	1.885(3)
O3	1.971(3)	O8	2.200(3)
Mean	1.835	Mean	1.888
Al3-O10A	1.801(3)	Al4-O12	1.723(3)
O9	1.856(2) ×2	O1	1.754(3)
O8	1.864(3)	O11	1.831(2) ×2
O10A	1.894(3)	O2	2.213(3)
Mean	1.854	Mean	1.870
Al3-O10B	1.464(1)		
AlO$_6$ Octahedra			
Al5-O12	1.816(2)	Al6-O8	1.857(2) ×2
O13	1.846(2)	O7	1.894(2) ×2
O3	1.859(2)	O15	1.953(2) ×2
O14	1.910(2)	Mean	1.901
O9	1.947(2)	Al7-O2	1.858(2) ×2
O4	2.025(2)	O6	1.886(2) ×2
Mean	1.900	O11	1.926(2) ×2
		Mean	1.890
SiO$_4$ and BO$_4$ Tetrahedra			
Si-O5	1.615(1)	O4-Si-O6	108.0(1) ×2
O4	1.635(2) ×2	O4-Si-O4	108.9(1)
O6	1.637(3)	O5-Si-O6	109.9(1)
Mean	1.630	O4-Si-O5	111.0(1) ×2
		Mean	109.5
B2-O13	1.439(5)	O10A-B2-O13	104.1(3)
O10A	1.469(5)	O7-B2-O10A	107.4(2) ×2
O7	1.470(3) ×2	O7-B2-O7	109.3(3)
Mean	1.462	O7-B2-O13	114.1(2) ×2
		Mean	109.4
BO$_3$ Triangles			
B1-O15	1.364(5)	O9-B1-O9	1l8.8(3)
O9	1.397(3) ×2	O9-Bl-O15	120.6(2) ×2
Mean	1.386	Mean	120.0
B3-O14	1.351(5)	O11-B3-O11	118.3(3)
O11	1.379(3) ×2	O11-B3-O14	120.8(2) ×2
Mean	1.370	Mean	120.0

termined by X-ray diffraction. To determine whether the actual symmetry is lower, we attempted to obtain electron diffraction patterns and TEM images in which twin or antiphase domains, which would reflect a lower symmetry, would be directly observable. Material from both the Larsemann Hills and Almgjotheii, Rogaland, Norway, was studied, but neither diffraction patterns nor images with meaningful contrast could be obtained, apparently because of rapid beam damage (H. Dong, personal communication).

Conversion to anisotropic displacement factors in the model with space group *C*2/*m* led to final residuals of 0.026 and 0.035. Additional details of the data measurement and structure refinement procedures are given in Table 2. The final refined values of the atomic positional parameters are listed in Table 3, the anisotropic displacement factors in Table 4[1], structure factors in Table 5[1], and selected interatomic distances and angles in Table 6.

DESCRIPTION OF THE STRUCTURE

AlO$_6$ and AlO$_5$ polyhedra

The principal features of the structure are illustrated in Figure 1. Atoms Al5, Al6, and Al7 have well-defined octahedral coordination, and the octahedra share edges to form the infinitely extended octahedral chains along [010] which are common to all members of the group described above. Al1, Al2, Al3, and Al4 have fivefold coordinations which, to a first approximation, are trigonal bipyramids. This feature implies a close relation to the andalusite structure, in which the interchain Al-polyhedra have similar trigonal bipyramidal coordination, and to the structure of werdingite in which only some of the interchain polyhedra have this coordination (see below). For the Al4O$_5$ polyhedron, however, the cation is significantly shifted out of the equatorial plane of the trigonal bipyramid toward one apical vertex. This results in one distance (Al4 – O2 = 2.213(3) Å) being very large compared to the other four (1.723 to 1.831 Å). To a first approximation, the Al4 polyhedron is therefore a distorted tetrahedron. The O-Al4-O angles range from 99.9° to 122.5°, with an average of 109.1°, compared to the ideal tetrahedral value of 109.47°. The shift of Al4 can be rationalized in terms of local charge balance; i.e., Al4 is bonded to O12, whose ideal valence sum (Pauling type, unadjusted for distances) has a very small value, 1.6 v.u. A reasonable empirical valence of 2.10 v.u. (Table 7) is achieved through shifts of Al4 and two Al5 atoms to positions much closer to O12, with distances $^{[5]}$Al4-O12 = 1.723(3) Å and $^{[6]}$Al5-O12 =

---

[1] For a copy of Table 4 and Table 5, Document AM-99-013, contact the Business Office of the Mineralogical Society of America (see inside front cover of recent issue) for price information. Deposit items may also be available on the American Mineralogist web site at http://www.minsocam.org or current web address.

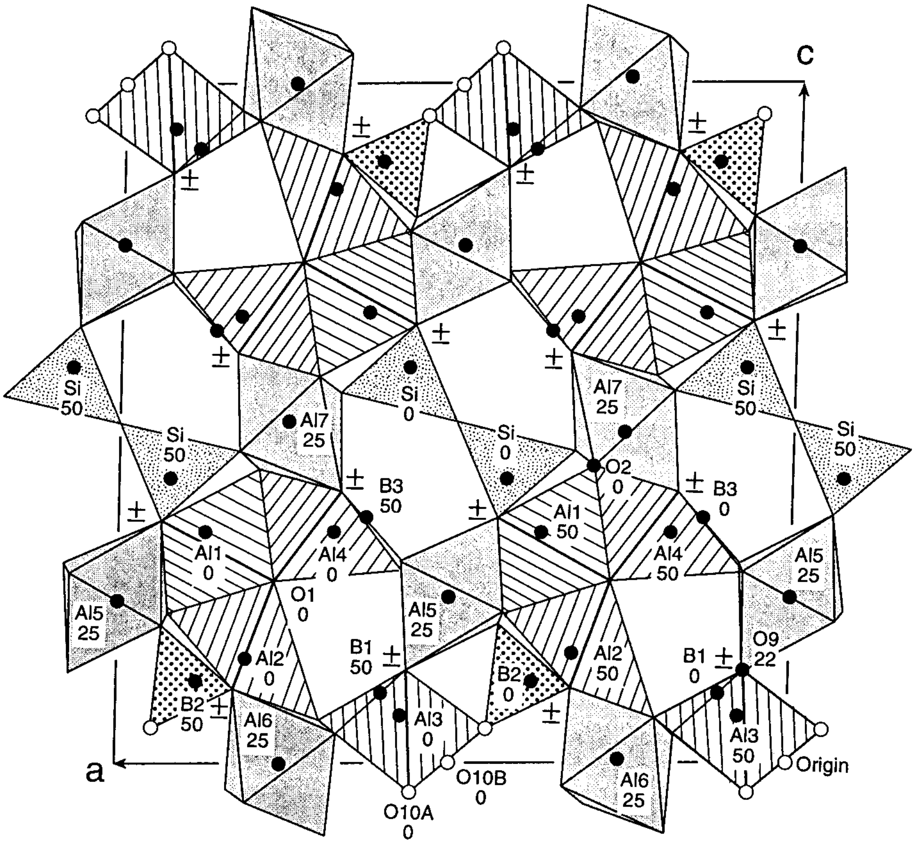

FIGURE 1. Projection of cation coordination polyhedra onto (010), for atoms in the range $y = 0$ to 1/2. Mirror planes at $y = 0$ and 1/2 repeat Al5, Al6, and Al7 octahedra (fully shaded) to form chains of edge-sharing octahedra as in sillimanite and related structures. Pairs of Si tetrahedra (fine stippling) share one vertex to form disilicate groups. B1 and B3 triangles plot as edge-views in this projection and hence are represented as single lines. Al trigonal bipyramids (lined) alternate along **b** with $^{[4]}$Si, $^{[3]}$B1, $^{[4]}$B2, and $^{[3]}$B3 polyhedra. The "±" symbols adjacent to some polyhedral vertices denote two superimposed anions.

1.816(2) Å, producing the shortest fivefold- or sixfold-coordinated Al-O distances in the structure. However, omission of O2 from the coordination sphere of Al4 leaves Al4 slightly underbonded, with a valence sum of 2.80 v.u. These two atoms must therefore be regarded as weakly bonded to one another. Al1, Al2, and Al3 are also shifted from the centers of their respective trigonal bipyramids, but to a much lesser extent than Al4. Atom Al(5)1 of the werdingite structure has this same ambiguous fivefold- or fourfold-coordination (Niven et al. 1991).

The ideal valence sum of 1.75 v.u. for O13 is also conspicuously small and is compensated for in the same fashion as for O12. That is, the Al5-O13 (×2) and B2-O13 distances of 1.846(2) and 1.439(5) Å are, respectively, the second-shortest $^{[6]}$Al-O and the shortest $^{[4]}$B-O distances in the structure. This shortening of bond distances produces a satisfactory empirical valence sum of 2.01 v.u. for O13 (Table 7).

The Al1, Al2, and Al4 bipyramids form an edge-sharing trimer (Fig. 1), with O1 as their common vertex, as described in more detail below.

SiO_4, BO_3, and BO_4 polyhedra

Si is nearly ideally tetrahedrally coordinated, with a mean Si-O distance of 1.630 Å (Table 6). Vertex-sharing through O5 produces disilicate groups, which also occur in werdingite. The tetrahedra around Si in Figure 1 are drawn with only three vertices shown, the fourth, apical oxygen atoms being omitted as they plot beyond the diagram's limits of $y = 0$ to 1/2 and because they are exactly superimposed on O atoms that are plotted. The bridging O5 anion of the disilicate group in boralsilite occupies an inversion center, requiring the Si-O-Si angle to be 180°. The rarity of this configuration in silicate structures raises the possibility that the symmetry is less than that of space group *C*2/*m*, but as noted above we have been unable to confirm such a relation.

Both werdingite and boralsilite would be classified as sorosilicates based on the existence of the disilicate group in each, but if the tetrahedrally coordinated B of boralsilite and Al of werdingite are included in the classification scheme, the structures can be viewed as having both single and double tetrahedra.

Boron occurs in both trigonal planar coordination (for B1 and B3) and tetrahedral coordination (for B2). Mean B-O distances are 1.462, 1.386, and 1.370 Å for the $B2O_4$ tetrahedron, $B1O_3$ triangle, and $B3O_3$ triangle, respectively, and the polyhedra approach their ideal shapes, the O-B1-O and O-B3-O angles summing to 360° in each case. In Figure 1, the B1 and B3 coordinating triangles are incomplete. The triangles are oriented with plane normal to (010), and the upper and lower vertices of the B1 and B3 triangles, respectively, are not shown as they are situated beyond the limits ($y = 0$ to 1/2) of the diagram; i.e., the triangles appear as edge views in this projection.

TABLE 7. Empirical bond-valence sums (v.u.)

	Al1	Al2	Al3	Al4	Al5	Al6	Al7	Si	B1	B2	B3	$\Sigma\underline{v}_a$
O1	0.61	0.68		0.76								2.05
O2	0.63			0.22			0.57 x2↓					
1.99												
O3	0.42	0.53			0.57 x2							2.09
O4	0.71 x2↓				0.36			0.97 x2↓				2.04
O5								1.03 x2				2.06
O7		0.71 x2↓			0.52 x2↓				0.77 x2↓		2.00	
O9			0.57 x2↓		0.45				0.93 x2↓			1.95
O10A			0.67, 0.52							0.77		1.96
O10B			0.78 $\overrightarrow{x2}$									1.56
O11				0.61 x2↓			0.48 x2↓				0.98 x2↓	2.07
O12				0.82	0.64 $\overrightarrow{x2}$							2.10
O13					0.59 $\overrightarrow{x2}$					0.83		2.01
O14					0.50 $\overrightarrow{x2}$						1.06	2.06
O15						0.44 x2			1.02			1.90
$\Sigma\underline{v}_c$	3.08	2.86	2.89	3.02	3.11	3.06	3.16	3.94	2.88	3.14	3.02	

Note: Bond-valences were calculated using the constants of Brese and O'Keeffe (1991).

Unoccupied polyhedra

An unoccupied trigonal bipyramidal site, defined by O1, O8, O9 (×2), and O12, completes a potential tetramer around O1. The vacancy appears as conspicuous "blank" areas adjacent to O1 in Figure 1. This potential cation site cannot be occupied by Al^{3+} because O1 would then be overbonded (4×0.6 v.u.). It might accommodate a low-valence cation, in which case the Pauling bond valence sum to O1 would assume its ideal value of 2 v.u. ($3 \times 0.6 + 0.2$). The only candidate among the elements analyzed by Grew et al. (1998) is Li^+, but Li_2O contents do not exceed 0.002 wt%.

Two other vacant sites which have a potential for cation occupancy can be discerned, both of which lie in the "blank" areas adjacent to the Si_2O_7 groups in Figure 1. One is a tetrahedral site defined by O5, O6, and O11 (×2); the other is an octahedral site defined by O4 (×2), O11 (×2), O5, and O12. Neither can be occupied as long as the existing double tetrahedron is a disilicate group, as this would result in tetrahedral edge-sharing and gross overbonding of O5 (the shared vertex of the double tetrahedron).

Octahedral chains and interchain units

The space between AlO_6 octahedral chains is occupied by trigonal bipyramids (Al1, Al2, Al3, and Al4), tetrahedra (Si, B2), and triangles (B1 and B3). Some descriptions of related structures have emphasized chains of such polyhedra extending parallel to the chains of octahedra. As a basis for comparison with related structures, equivalent relations are described here for boralsilite. Figure 1 shows that there are four such cross-linking chains of polyhedra in boralsilite, each of which shares vertices with the chain of Al5 octahedra. They consist of (1) B1 triangles and Al3 trigonal bipyramids linking Al5 octahedra to Al6 octahedra, (2) B2 tetrahedra and Al2 trigonal bipyramids linking Al5 octahedra to Al6 octahedra, (3) Si tetrahedra and Al1 trigonal bipyramids linking Al5 octahedra to Al7 octahedra, and (4) B3 triangles and Al4 trigonal bipyramids linking Al5 octahedra to Al7 octahedra. The individual chains of polyhedra are illustrated in Figures 2 through 5. In all of these projections, alternate chains of AlO_6 octahedra differ in coordinates by 1/4 in the projection direction. Because the shapes of the distorted trigonal bipyramids are complex and difficult to visualize in these projections, Al1 through Al4 trigonal bipyramidal polyhedra are not shown (except in Fig. 1) and are represented only by their central Al atoms.

In all four units, Al in trigonal bipyramidal coordination alternates in the [010] direction with some other cation, i.e., with B1 triangles, B2 tetrahedra, Si tetrahedra, and B3 triangles in the cases of polyhedral chains 1 through 4, respectively (Figs. 2–5). Whether cations are tetrahedrally or trigonally coordinated, two vertices are oriented to form an edge parallel to *b* that bridges the apical vertices of adjacent Al octahedra in one chain of octahedra. A third vertex is shared with an adjacent chain of octahedra, thus linking chains together. For the B2 and Si tetrahedra, the fourth vertex is shared with another chain of polyhedra, creating a disilicate unit in the case of Si. The ability of the same backbone of octahedral chains to play a similar role in such a variety of aluminoborosilicates (Table 1) is in part based on the ability of different B, Si, and Al tetrahedra and B triangles to link chains in equivalent ways. The distortions existing in those shared polyhedra create sites of various geometries with coordinations of 3, 4, 5, or 6 which can be occupied, in part, by Al or B, two cations which are unusual in their ability to adopt very different coordinations in the same structure. The coordination of Al4, which is intermediate between fourfold and fivefold, especially illustrates the ability of Al to adjust to the structure topologies defined by AlO_6 octahedra and by the B and Si symmetrical polyhedra.

The diagrams cited above suggest a convenient way to view the structures of boralsilite and related compounds. That is, the basic structural unit in boralsilite can be viewed as a "pinwheel" of which the chain of Al5 octahedra forms the central axis. Each of the four kinds of polyhedral chains, plus the other chains of AlO_6 octahedra to which those polyhedral chains bridge, can be viewed as the wings of the pinwheel. For example, Figure 1 shows that one wing of the pinwheel consists of the polyhedral chain of alternating B1 triangles and Al3 trigonal bipyramids, plus the Al6 chain of octahedra.

Solid solution involving the O10A and O10B sites: The question of "paraboralsilite"

As described above, refined parameters imply that there are approximately 0.20 vacancies per unit cell for O10A, which

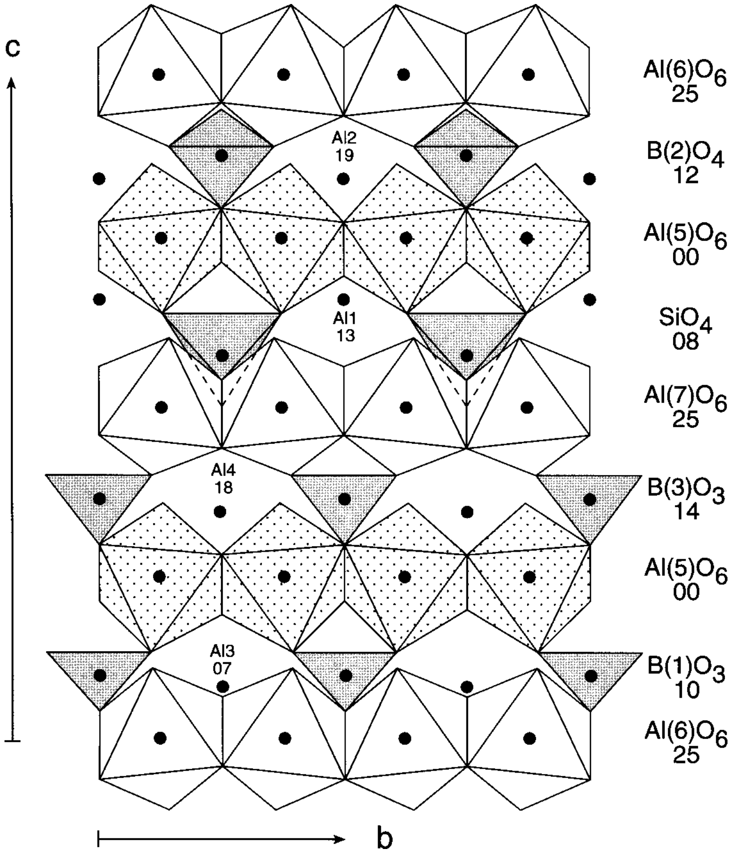

FIGURE 2. Projection onto (100) of cation coordination polyhedra in the range $x = 0$ to 1/4. Alternate chains of Al5 and Al6 octahedra differ in height along *a* by 1/4, with those at a lower level being stippled and those at an upper level being unmarked. They are cross-linked successively by chains of $^{[5]}$Al3-$^{[3]}$B1, $^{[5]}$Al4-$^{[3]}$B3, $^{[5]}$Al1-$^{[4]}$Si, and $^{[5]}$Al2-$^{[4]}$B2 polyhedra. To improve clarity, only the positions of the $^{[5]}$Al1 through $^{[5]}$Al4 atoms are shown, without the outlines of their trigonal bipyramidal coordination polyhedra.

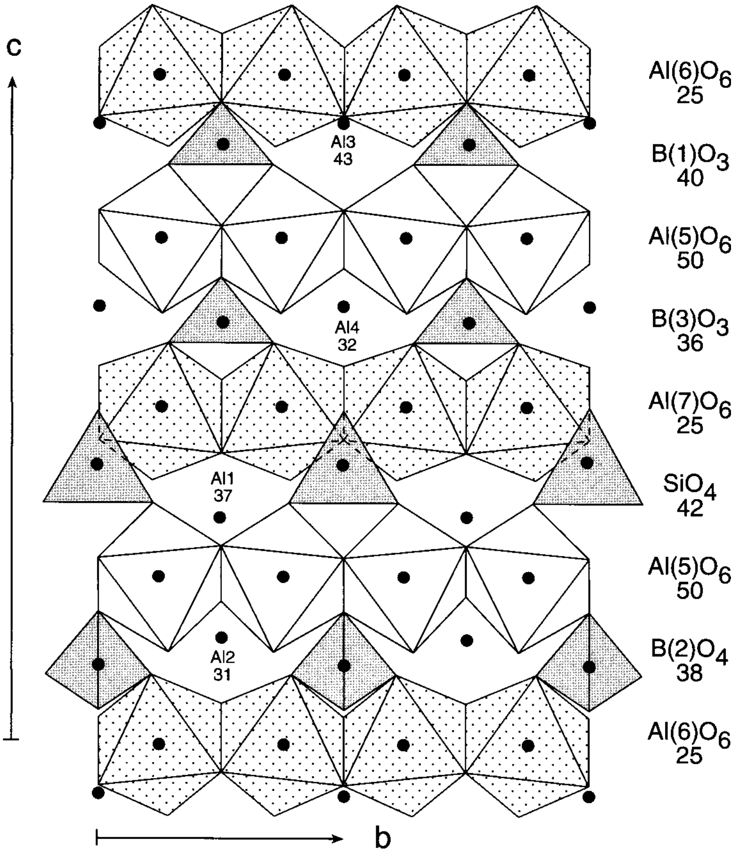

FIGURE 3. Projection onto (100) of cation coordination polyhedra in the range $x = 1/4$ to 1/2.

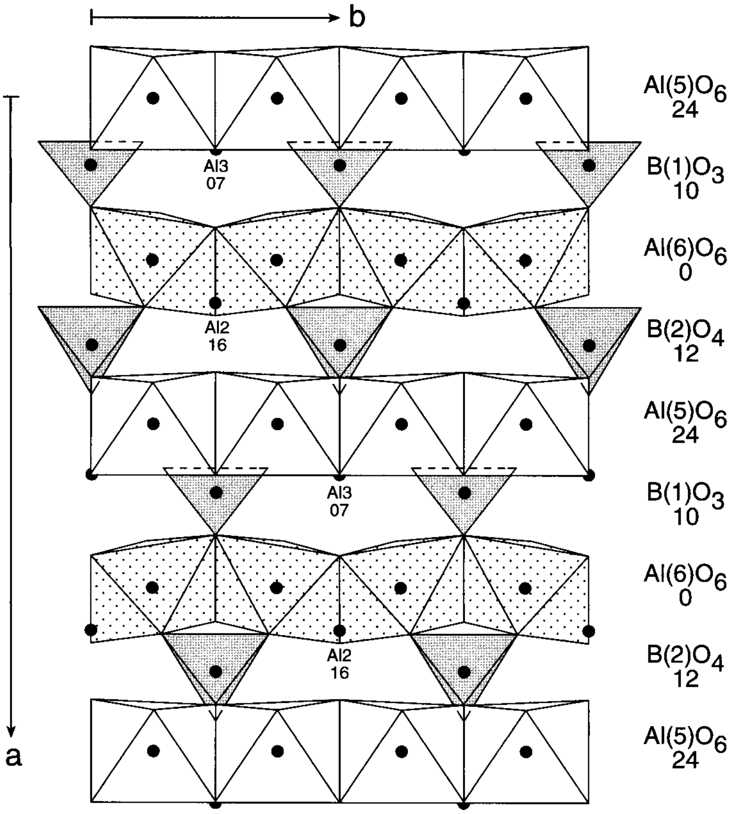

FIGURE 4. Projection onto (001) of cation coordination polyhedra in the range $y = 0$ to 1/4.

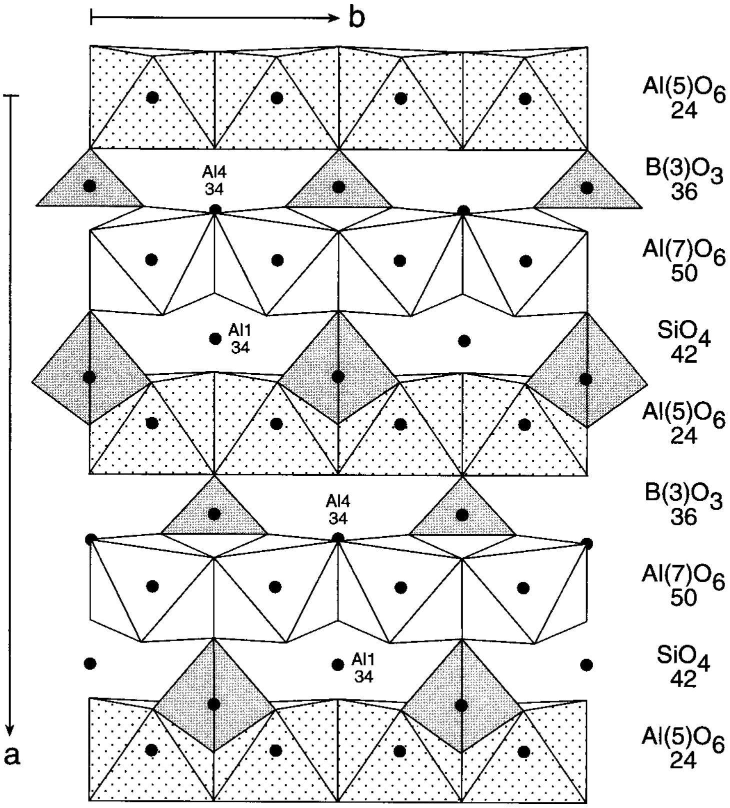

FIGURE 5. Projection onto (001) of cation coordination polyhedra in the range $y = 1/4$ to 1/2.

occupies equipoint 4*i*. This is coupled with evidence for partial occupancy of site O10B, on equipoint 2*b*, the magnitude of the occupancy (0.29 atoms) approximately matching the number of vacancies on O10A, within error. When the occupancies of the two sites were initially constrained to sum to a total of four oxygen atoms, the occupancy of O10A refined to 3.75(2), with that of O10B constrained to be 0.25. The results of the independent refinements for the two sites (3.80 and 0.29) are preferred as they contain no assumptions about the total number of atoms present, but the results of both kinds of refinement are the same within three esd's.

Al3 occupies the trigonal bipyramid of which O10A is a vertex. Assuming that O10B is occupied rather than O10A, the Al3-O10B distance is 1.464 Å, a value which is almost identical to the mean B-O distance for the tetrahedrally coordinated B2 site. This implies the possibility of B on the Al3 site. Such a model entails (1) substitution of B^{3+} for Al^{3+} on Al3, hereafter denoted by Al3(Al) → Al3(B); (2) occupancy of O10B coupled with a vacancy on O10A, the two sites being too close together for simultaneous occupancy; (3) a change in coordination from trigonal bipyramidal for Al3(Al) to tetrahedral for Al3(B), and (4) a simultaneous change of coordination from tetrahedral to trigonal planar for B2, a change necessitated by the deletion of one of its ligands, O10A.

Figure 6 shows the result of the above changes. Omission of O10A in favor of O10B leaves Al3(B) coordinated by O8, O9 (×2), and O10B at the vertices of a flattened tetrahedron. This distorted tetrahedron could easily be made more nearly regular and the long Al3-O8 and Al3-O9 distances of 1.864 and 1.856 Å, respectively, shortened to values appropriate for $^{[4]}$B-O bonds by shifts in positions of O8 and O9, and/or Al3(B). Likewise, the change in coordination number from four to three for B2 could be easily accomplished by a small shift of B2 from the current tetrahedrally coordinated site into the plane of the (former) tetrahedron face defined by O7 (×2) and O13.

The result of full occupancy of O10B rather than O10A gives rise to a structure (Fig. 6) for which the term "paraboralsilite" is introduced to distinguish it from the unmodified boralsilite structure. Because the O10B site is an inversion center, the $Al3(B)O_4$ tetrahedron must share its O10B vertex with an identical tetrahedron, forming a diborate group, B_2O_7. Adjacent diborate groups are linked parallel to *b* by $B1O_3$ triangles (Figs. 3 and 4), one triangle being associated with each tetrahedron by sharing common vertices, O9. The result is stepladder-like chains along [010], the B_2O_7 groups forming the steps and the connecting BO_3 groups the sides of the ladders. There is ample precedent for diborate groups in "paraboralsilite," as these entities occur in a number of other borosilicate structures, e.g., taramellite (Mazzi and Rossi 1980), nagashimalite (Matsubara 1980), hellandite (Mellini and Merlino 1977), and tadzhikite (Chernitsova et al. 1982). There is also precedent for the presence of both diborate and disilicate groups in the same structure, that being in the structure of danburite (Phillips et al. 1974), but there the groups are linked into a three-dimensional feldspar-type framework, whereas they are not so linked in hypothetical "paraboralsilite."

The solid solution (Al,B) inferred for the Al3 site and its association with the "split" atom pair O10A and O10B has a partial analogy in the structure of werdingite. Niven et al. (1991) proposed (Al,B) solid solution on the Al(4)2 site coupled to

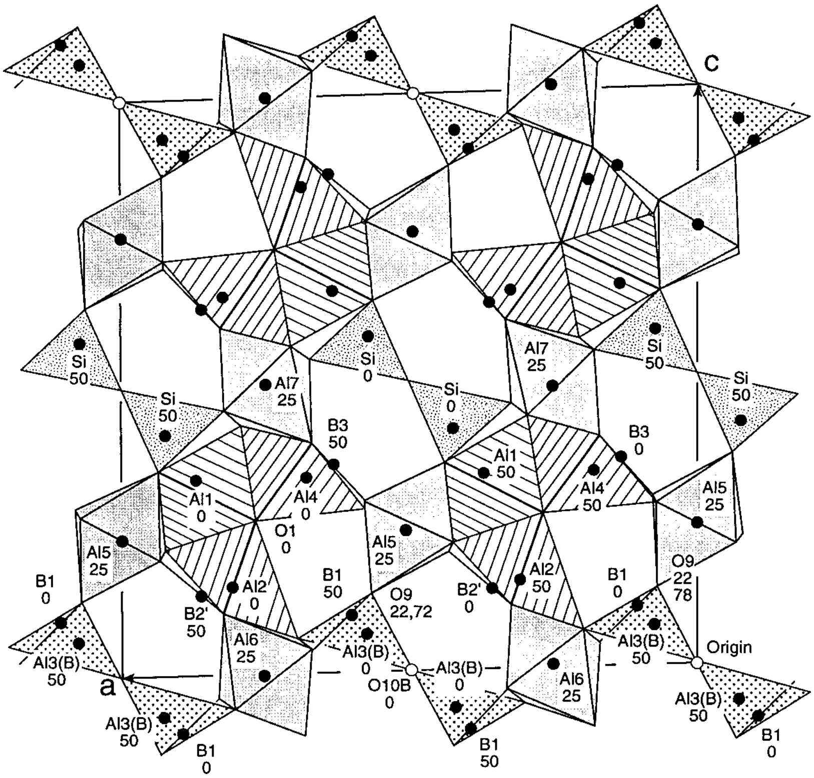

FIGURE 6. Projection of cation coordination polyhedra on (010) for the hypothetical end-member "paraboralsilite" structure. $^{[4]}$B [denoted as "Al3(B)"] has replaced $^{[5]}$Al3 to form diborate tetrahedral groups, and $^{[4]}$B2 has become $^{[3]}$B2 owing to the loss of one ligand, 010A.

alternate occupancy of the "split" anion sites O19A and O19B. In werdingite the cation substitution involves a change in coordination from tetrahedral Al(4)2[Al] [meaning: Al(4)2 site occupied by Al] to trigonal planar B(3)2(≈Al(4)2[B]), as opposed to the change from trigonal bipyramidal Al3(Al) to tetrahedral Al3(B) in boralsilite. The positions of Al(4)2 and B(3)2 are slightly different in werdingite, i.e., another "split" atom pair. It is conceivable that the same is true of Al3(Al) and Al3(B) in boralsilite, but we have no evidence of this from refined parameters, including temperature factors, owing perhaps to the minute amount of scattering power involved.

Because O10A and O10B occupy four-fold and two-fold equipoints, respectively, "paraboralsilite" will contain only 72 anions/cell and the formula $Al_{28}B_{16}Si_4O_{72}$ will not be charge-balanced ($\Sigma\, v_c = +148$ and $\Sigma\, v_a = -144$ v.u.). One solution to the problem would be replacement of Al^{3+} on one of the fourfold octahedral sites (Al6 or Al7) with Fe^{2+}. Indeed, electron microprobe analyses of Larsemann Hills boralsilite gave 0.26 to 0.51 wt% Fe as FeO, equivalent to 0.042 to 0.081 Fe apfu. The required substitutions would be as shown in Table 8.

Depending on the extent of solid solution, these substitution mechanisms can be summarized as $8Al^{3+} + 4O^{2-} + 2\square \rightarrow 4B^{3+} + 4Fe^{2+} + 2O^{2-} + 4\square$ or $4Al^{3+} + O^{2-} \rightarrow 2B^{3+} + 2Fe^{2+} + \square$.

A second possible solution to the problem of overall charge imbalance involves replacement of all four Si^{4+}/cell with B^{3+} or Al^{3+}; this replacement is suggested by the deficiency of Si in the analyses of the Larsemann Hills boralsilite (Grew et al. 1998). The charge-balanced formula would be $Al_{28}B_{20}O_{72}$ or $Al_{32}B_{16}O_{72}$ and the substitutions could be expressed as follows, e.g., for B^{3+} substitution:

$4Al^{3+} + 4Si^{4+} + 4O^{2-} + 2\square \rightarrow 4B^{3+} + 4B^{3+} + 2O^{2-} + 4\square =$
$4B3 + 4B^{3+} + 2O^{2-} + 4$
or
$2Al^{3+} + 2Si^{4+} + O^{2-} \rightarrow 4B^{3+} + \square = 4B^{3+} +$.

Given the substitutions suggested above, the composition of the Larsemann Hills sample reported by Grew et al. (1998) can be interpreted as end-member boralsilite $Al_{16}B_6Si_2O_{37}$ with minor solid solution of "paraboralsilite." The average composition of the Larsemann Hills sample, assuming B + Si = 8 apfu and Fe = Fe^{2+}, yields a formula $Fe_{0.08}Al_{15.97}B_{6.08}Be_{0.002}Si_{1.92}O_{37}$. If this formula were normalized to 24 cations instead of 37 O atoms, the total cation charge would be 73.836, not significantly different than the 73.8 negative charges calculated from occupancy of O10A and O10B, i.e., $Fe_{0.08}Al_{15.92}B_{6.08}Be_{0.002}Si_{1.92}O_{36.92}$. This formula is equivalent to 92% $Al_{16}B_6Si_2O_{37}$ and 8% of a "paraboralsilite" end-member $FeAl_{15}B_7SiO_{36}$ (ignoring Be).

The solid solutions suggested above are only two examples of the flexibility inherent in the structures of the family of boroaluminosilicates, sillimanite, and andalusite with a backbone of AlO_6 edge-sharing chains. The position of boralsilite in this family and comparison of the interchain units in each member of this family are discussed in the next section.

TABLE 8. Substitutions which transform boralsilite into the hypothetical phase "paraboralsilite"

	boralsilite	"paraboralsilite"
Cell contents	$Al_{32}B_{12}Si_4O_{74}$	$Fe_4Al_{24}B_{16}Si_4O_{72}$
Al3	$4Al^{3+}$	$4B^{3+}$
Al6 (or Al7)	$4Al^{3+}$	$4Fe^{2+}$
O10A	$4O^{2-}$	$4\square$
O10B	$2\square$	$2O^{2-}$

Interchain units in related structures

Types of interchain units. The polyhedral chains in boralsilite described above, consisting of four different sequences of alternating cations, are parallel to and cross-link the chains of edge-sharing octahedra. The relations between polyhedra can be described in an alternative, convenient way, however, such that there are four different kinds of interchain unit. Each of these occupies the space between four $^{[6]}$Al chains which form a square in projection down *b*. Four such interchain units that fill the four "squares" around any given central Al5 octahedron (Fig. 1). These units consist of the following components, numbered in sequence around Al5:

Unit 1: Si_2O_7 dimer.

Unit 2: A core consisting of an Al2-Al1-Al4 trimer of edge-sharing trigonal bipyramids, augmented by the B3 triangle and B2 tetrahedron joined above (and below) along *b*.

Unit 3: A core consisting of an Al3-Al3 dimer of edge-sharing (shared edge spanning an inversion center at 1/2, 0,0) trigonal bipyramids, joined above (and below) along *b* by two B1 triangles and laterally to two B2 tetrahedra.

Unit 4: Identical to unit 2.

Andalusite. The andalusite structure has only one kind of interchain unit. It consists of a central dimer of two edge-sharing Al trigonal bipyramids and in that sense it is similar to unit 3 of boralsilite. It differs, however, in being joined above, below, and laterally by six vertex-sharing, isolated Si tetrahedra.

The length of the shared edge of the trigonal bipyramids in andalusite is exceptional in being only 2.23 Å, near the very small O-O distance typical of a CO_3 group, as brought to our attention by C.W. Burnham (personal communication). Of the three shared bipyramid edges in the boralsilite structure, only that for the dimer (O10A-O10A) is remarkable, being 2.256(6) Å, whereas those for the trimer (O1-O3 and O1-O2) are 2.463(4) and 2.541(4) Å, respectively. The correspondence with the short dimer edge of andalusite emphasizes the equivalence of the dimers in the two structures.

Werdingite. The werdingite structure has a variety of interchain units involving B in triangular coordination, tetrahedral Si and Al, and Al in trigonal bipyramidal coordination. It differs from boralsilite in having no tetrahedral B, having (Mg,Fe^{2+}) in trigonal bipyramidal coordination, and in having substitution of Fe^{3+} for $^{[4]}$Al. One of the several kinds of interchain units is analogous to the trimer of unit 2 above. It consists of three edge-sharing bipyramids, two of which are occupied by Al[Al5(1) and Al5(2)] and one by (Mg,Fe). Whereas the trimer in boralsilite is joined above and below to a B3 triangle and a B2 tetrahedron, that in werdingite is joined only to B(3) triangles.

Sillimanite. The sillimanite structure has interchain units of only one type, tetrahedral (Al,Si) dimers which share vertices to form a double chain of tetrahedra which parallels and links the octahedral chains. Unit 1 in boralsilite, the tetrahedron dimer, is analogous to the dimer in sillimanite, but the Si dimers of boralsilite alternate with Al bipyramids in the chain direction, rather than with a second tetrahedral dimer as in sillimanite. A further analogy lies in the distribution of pairs of vertex-sharing tetrahedra that occupy adjacent interchain units along **a** of boralsilite with periodicity *a*/2. Tetrahedral dimers in adjacent interchain units share trans vertices of the Al7 octahedron. In boralsilite there is thus a slab of structure parallel to (100) consisting of chains of Al octahedra alternating with tetrahedral dimers and Al1 bipyramids. In sillimanite, the corresponding (100) slab consists of chains of Al octahedra alternating with tetrahedral dimers, which are linked to form double chains of tetrahedra. In werdingite there is a double chain of tetrahedra [Si(4)1,Si(4)2,Al(5)2, and Fe/Al(4)1; Fig. 2 of Niven et al. (1991)] similar to that of sillimanite, except that two opposite [Al(5)2] tetrahedra do not share a vertex to form a dimer.

Grandidierite. The grandidierite structure has only one type of interchain unit, consisting of a dimer of edge-sharing $^{[5]}Al(Mg,Fe)O_8$ trigonal bipyramids. This dimer alternates in the chain direction with an isolated SiO_4 tetrahedron and an isolated BO_3 triangle. The corresponding unit in boralsilite consists of the edge-sharing Al1 and Al4 bipyramids (but not Al2) and the B3 triangle and Si tetrahedron. This unit can also be viewed as consisting of parallel chains of alternating Al4 bipyramids and B3 triangles and of Al1 bipyramids and Si tetrahedra (Figs. 2 and 3).

Synthetic $Al_{18}B_4O_{33}$. The structure of $Al_{18}B_4O_{33}$ also has only one type of interchain unit, which consists of an edge-sharing dimer of Al bipyramids alternating with an isolated AlO_4 tetrahedron plus an isolated BO_3 triangle. The corresponding unit in boralsilite consists of B3, Al4, Al1 and Si polyhedra; the major difference between it and $Al_{18}B_4O_{33}$ is in the absence of Si in $Al_{18}B_4O_{33}$. As with grandidierite, such units are knit together through tetrahedral linkages between two units, the pattern of vertex sharing being different in grandidierite and $Al_{18}B_4O_{33}$.

DISCUSSION

This study was initiated in the expectation that this family of related boroaluminosilicates would have structures which, when compared with one another, could be shown to have a small number of subunits, the relative proportions of which would vary in a regular way and provide a simple rationale for trends in composition; i.e., as in a polysomatic series. This has not proven to be the case, although there are some simple general themes and common structural elements as described above. Rather, the variety of interchain units and resulting compositions is seen to be a result of an unusually diverse combination of cation charges and coordination polyhedra. Boron may be present in tetrahedral or plane triangular coordination. The value of the Pauling-type bond valence for the latter situation is +1 v.u., thus providing a means of substitution of B^{3+} for Si^{4+}, with loss of one tetrahedral vertex. Al occurs in three different coordinations: tetrahedral, trigonal bipyramidal, and octahedral (in edge-sharing chains only). Thus Al may take the place of $^{[4]}Si$, but (Mg,Fe^{2+}) may take the place of Al^{3+}. All polyhedra have dimensions which permit interchange to some degree, the trigonal bipyramidal polyhedra being especially flexible. The existence of partial site occupancies in the structures of werdingite, mullite, boralsilite, and $Al_{18}B_4O_{33}$ further offers potential mechanisms for solid solutions, as those partial occupancies represent local occurrences of units other than the average ones. Such variance may occur in both an ordered and disordered fashion. Lastly, we have identified unoccupied sites in the boralsilite structure for which coordination numbers and distances are not much different than values for occupied sites. The backbone of $^{[6]}Al$ chains thus provides an unusually flexible framework for a variety of interchain units. Other variants of these structural schemes may be expected therefore, and if TEM can be used to image material without beam damage, a variety of ordered and disordered relations involving interchain units may be observed.

ACKNOWLEDGMENTS

We are grateful to Hailiang Dong for his attempts to obtain TEM data on boralsilite, and to David Waters and Associate Editor Lee Groat for their throughtful and helpful reviews. This is contribution no. 510, from the Mineralogical Laboratory, Department of Geological Sciences, The University of Michigan, Ann Arbor, Michigan 48109.

REFERENCES CITED

Angel, R.J. and Prewitt, C.T. (1986) Crystal structure of mullite: A re-examination of the average structure. American Mineralogist, 71, 1476–1482.

Brese, N.E. and O'Keeffe, N. (1991) Bond-valence parameters for solids. Acta Crystallographica, B47, 192–197.

Burnham, C.W. (1963) Refinement of the crystal structure of kyanite. Zeitschrift für Kristallographie, 118, 337–360.

Burnham, C.W. and Buerger, M.J. (1961) Refinement of the crystal structure of andalusite. Zeitschrift für Kristallographie, 115, 269–290.

Chernitsova, N.M., Pudovkina, Z.V., and Pyatenko, Yu.A. (1982) The crystal structure of tadzhikite $(Ca,Tr)_4(Y,TR)_2(Ti,Fe,Al)(O,OH)_2$ $[Si_4B_4O_{22}]$. Doklady Akademii Nauk SSSR, 264, 342–344 (in Russian).

Garsche, M., Tillmanns, E., Almen, H., Schneider, H. and Kupcik, V. (1991) Incorporation of chromium into aluminium borate $9Al_2O_3{\cdot}2B_2O_3(A_9B_2)$. European Journal of Mineralogy, 3, 793–808.

Grew, E.S., McGee, J.J., Yates, M.G., Peacor, D.R., Rouse, R.C., Huijsmans, J.P.P., Shearer, C.K., Wiedenbeck, M., Thost, D.E., and Su, S-C. (1998) Boralsilite $(Al_{16}B_6Si_2O_{37})$: A new mineral related to sillimanite from pegmatites in granulite-facies rocks. American Mineralogist, 83, 638–651.

Ihara, M., Imai, K., Fukunaga, J., and Yoshida, N. (1980) Crystal structure of boroaluminate, $9Al_2O_3\sum B_2O_3$. Yogyo-Kyokai-Shi, 88(2), 28–34 (in Japanese with English abstract).

Matsubara, S. (1980) The crystal structure of nagashimalite, $Ba_4(V^{3+},Ti)_4$ $[(O,OH)_2|Cl|Si_8B_2O_{27}]$. Mineralogical Journal (Tokyo), 10, 131–142.

Mazzi, F. and Rossi, G. (1980) The crystal structure of taramellite. American Mineralogist, 65, 123–128.

Mellini, M. and Merlino, S. (1977) Hellandite: A new type of silicoborate chain. American Mineralogist, 62, 89–99.

Niven, M.L., Waters, D.J., and Moore, J.M. (1991) The crystal structure of werdingite, $(Mg,Fe)_2Al_{12}(Al,Fe)_2Si_4(B,Al)_4O_{37}$, and its relationship to sillimanite, mullite, and grandidierite. American Mineralogist, 76, 246–256.

Phillips, M.W., Gibbs, G.V., and Ribbe, P.H. (1974) The crystal structure of danburite: A comparison with anorthite, albite, and reedmergnerite. American Mineralogist, 59, 79–85.

Sokolova, Ye.V., Aziz, A.V., Simonov, M.A., Leonyuk, N.I., and Belov, N.V. (1978) Crystal structure of synthetic ortho-3-borate $Al_5(BO_3)O_6$. Doklady Akademii Nauk SSSR, 243, 655–658 (in Russian).

Stephenson, D.A. and Moore, P.B. (1968) The crystal structure of grandidierite, $(Mg,Fe)Al_3SiBO_9$. Acta Crystallographica, B24, 1518–1522.

Werding, G. and Schreyer, W. (1984) Alkali-free tourmaline in the system MgO-Al_2O_3-B_2O_3-SiO_2-H_2O. Geochimica et Cosmochimica Acta, 48, 1331–1244.

———(1996) Experimental studies on borosilicates and selected borates. In Mineralogical Society of America Reviews in Mineralogy, 33, 117–163.

MANUSCRIPT RECEIVED JANUARY 8, 1998
MANUSCRIPT ACCEPTED JANUARY 19, 1999
PAPER HANDLED BY LEE A. GROAT